www.amlett.com, www.vbripress.com/aml, DOI: 10.5185/amlett.2015.5645 Published online by the VBRI Press in 2015

Influence of particle velocities and impact angles on the erosion mechanisms of AISI 1018 steel

Paul C. Okonkwo[1], A. M. A. Mohamed[1, 2*], Essam Ahmed[2]

[1]*Center for Advanced Materials, Qatar University, 2713 Doha, Qatar*
[2]*Department of Metallurgical and Materials Engineering, Faculty of Petroleum and Mining Engineering, Suez University, 43721 Suez, Egypt*

[*]Corresponding author. E-mail: adel.mohamed@qu.edu.qa; madel@uqac.ca

Received: 21 March 2015, Revised: 20 May 2015 and Accepted: 05 June 2015

ABSTRACT

Failure of oil and gas pipeline due to solid particles entrainment has been a great concern to the petroleum industry. Erosion is the gradual material removal of pipeline materials due to solid particle impingement and results in unacceptable damage to the pipeline steel material surface. Because this process is difficult to investigate during operation, laboratory simulation test provides some insight. In this study, series of erosion tests were carried out to investigate the influence of particle velocity and impact angle on the erosion mechanism of AISI 1018 steel. Sand blaster erosion machine was used as the test equipment while the particle velocity and impact angle were ranged from 20 to 80 m/s and between 30 and 90° respectively. The results showed that at 90° impact angle, ploughing mechanism was operative, while material removal through low angle cutting was the dominant mechanism at lower impact angle during the erosion of AISI 1018 steel. Mainly, embedment of aluminium oxide particles on the target steel surface, micro–cutting, low angle cutting, pitting and ploughing were observed for low impact angle tests. It was suggested that scratches, cuttings and ploughing observed on some failed oil and gas pipeline steels could be attributed to erosion mechanism.

Keywords: AISI 1018 steel; oxide particles; impact angle; particles velocity; erosion mechanisms.

Introduction

Oil and gas transportation steel pipeline has been considered one of the effective means of transporting petroleum products from one region to another **[1, 2]**. Steels are used as medium for transporting those petroleum products as they are required to withstand high pressure, stress and environmental conditions **[3, 4]**.However, erosion of the steels has been a major form of failure experienced in the oil and gas industry and is often caused by the impingement of solid particles on the pipeline's surface **[5]**.Material removal due to solid particle erosion is believed to be a series of impact events that occur in pipelines and cause extensive damage due to change in the solid-liquid flow direction. The erosion of steel surface by stream of solid particles has been an issue of concern for decades due to high material loss and maintenance costs **[6, 7]**. Unfortunately, there is no universal model that can effectively predict all erosion situations **[8-10]**, and development of a reliable and effective model for solid erosion process still remains a challenge.

Several attempts have been made to understand the effect of different parameters, such as temperature, impact velocity, particles size, angle of attack and microstructure of both the impinging and eroding surface on the solid particles erosion process **[11-17]**.However, each parameter behaves peculiar to each process and is often complex due to interrelated variables involved **[18-24]**.Among these parameters, the particle velocity and impact angles play critical role in the erosion process **[25-28]**. Lindsley *et al.* **[27]** investigated the effect of particle velocity on erosion rate of two alloys of 70–30 brass and Fe–C martensite using an erosion tester. Their results revealed that erosion rate is dependent on velocity. The results also showed that while martensite material was eroded by cracking mechanism, brass material exhibited plastic deformation mechanism.

Matsumura et al. **[29]** conducted erosion tests of 304 stainless steel in order to investigate the effect of surface damage at different impacting angles due to impinging silica sand particle. Peak erosion rate was found between 30 and 50° for pure iron and 304 stainless steel. Finnie et al. **[6]**also reported that peak erosion and wear rate occurred between 15° and 40° for ductile materials. On the other hand, Stachwick et al. **[30]** showed that for brittle materials, erosion and wear rate increase with increasing impact angle reaching the peak at 90°. Bukhaiti et al. **[25]** investigated the effect of impingement angle on slurry

erosion behaviour of AISI 1017 steel and high-chromium white cast iron. Interestingly, their result revealed that different mechanisms occur at different impinging angles for the two different tested materials. Recently, Islam et al. **[17]** conducted erosion tests on API X42 steel material using aluminium oxide as impact solid particle. The result showed that at low abrasive feed rate, erosion rate decreases with increasing impact angle. Increased particle velocity resulted in increased erosion rate.

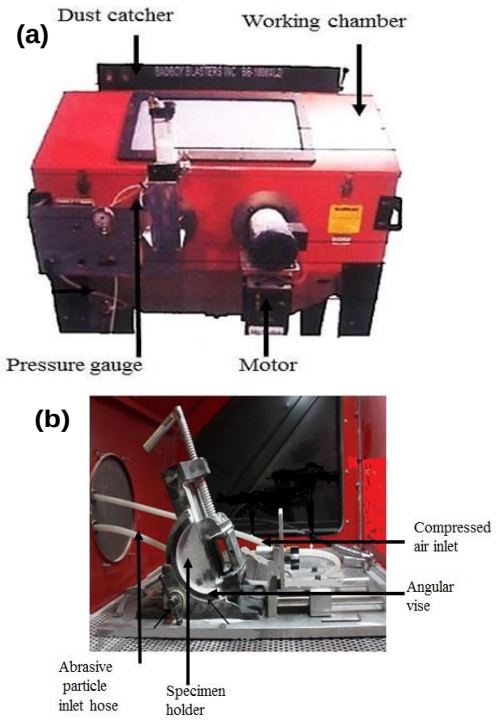

Fig. 1. (a) The external view and (b) internal view of the sand blaster erosion machine.

Based on the study carried out on different steel materials by several authors, erosion of steel materials can be classified according to their response to solid particle impingement at different impinging angles **[25, 26, 28, 31, 32]**. Ductile materials belong to the group that plastically deformed with maximum erosion rate at low impact angle, while brittle materials fracture with maximum erosion rate at normal impact angle. Despite several studies on the effects of impact angle and velocity on the solid particle erosion of these groups of materials **[19, 23, 33-35]** effort is still required to understand the erosion mechanism of material removal by solid particles. Many studies were done to explain the erosion mechanism of carbon steel materials used in transporting oil and gas is limited in literature. Further study on the effect of particle velocity on the erosion mechanism trend of AISI 1018 steel with respect to impact angle becomes necessary. The objective of this study is to explore the solid particle erosion mechanisms by which materials are removed from the target of AISI 1018 steel surface at various velocities and impact angles. The novelty of this study is to use sand blaster erosion machine to investigate the effect of solid sand particle velocity and impact angle on the erosion mechanism of AISI 1018 steel used in the transportation of oil and gas. The outcome of the study will provide a better understanding of the underlining mechanism responsible for failure of AISI 1018 steel used in the petroleum industry. This will enhance the application of better erosion control measure to reduce erosion of the steel pipeline materials.

Experimental

Test equipment

An in-house built type dry sand blaster erosion tester shown in **Fig. 1** was used to study the erosion behaviour of AISI 1018 steel impinged with aluminium oxide particles at room temperature. The equipment was designed to impinge the targeted sample surface with solid particles at different velocities under controlled erosion conditions. The erosion test facility consists of abrasive feed meter which acts as the reservoir tank and controls the feed rate of solid particles. Air flow meter, pressure gauge and specimen chamber are components incorporated in the design of the equipment.

Material

The aluminium oxide was used as received from Magnum Engineers, Peenya Industrial Estate, Bangalore, while the AISI 1018 steel material was supplied by Hebei Yineng Pipeline Group Co., Ltd., Shandong, China. The AISI 1018 steel samples used in these tests were cylindrical in shape of 15.8 mm diameter and 4.7 mm thickness. Prior to each test, the AISI 1018 steels were ground using 240, 320 and 600-grit silicon carbide papers, and subsequently polished using 1, 0.3 and 0.05µm gamma aluminium suspension. The chemical composition of the materials used in this study is given in **Table 1**.

Table 1. Chemical compositions of target material and impinging solid particles.

Material	Specimen	Chemical composition					
AISI 1018 steel	Target material	Fe	C	Mn	P	S	Si
		98.98	0.18	0.60	0.04	0.05	0.15
Aluminium oxide	Impinging solid particles	Al_2O_3	TiO_2	SiO_2	Fe	MgO	Alkali
		99.5	0.099	0.05	0.08	0.02	0.30

Scanning electron microscope (SEM) was used to characterise the morphology of the initial surface of the AISI 1018 steel and aluminium oxide samples used in this study. **Fig. 2(a)** and **(b)** show the microstructure of the AISI 1018 steel and average size of erodent aluminium oxide particles used in these tests, respectively.

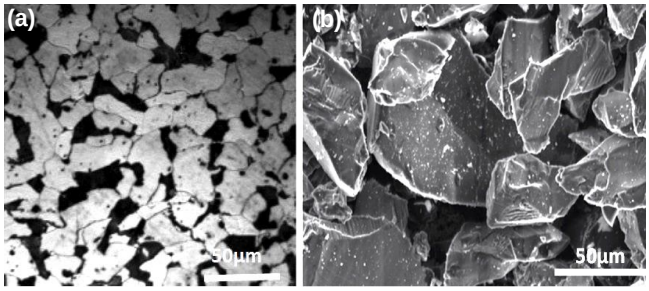

Fig. 2. Micrographs of: (a) AISI 1018 steel and (b) aluminium oxide particles size distribution.

Test procedure

The test equipment used to carry out the erosion tests is in accordance with specification of ASTM standard G76 **[36]**. Particle velocity was determined as a function of pressure using double disc method detailed elsewhere **[37]**, while the feed rate of the solid particles was determined by measuring the weight of the abrasive particles coming through the nozzle per unit time.

The aluminium oxide particles were forced through a nozzle by using a compressed air stream that caused the erodent to impinge the AISI 1018 steel surface at different velocities. The AISI1018 steel specimens were kept at impact angles of 30 and 90° for the two different test conditions. The stand-off distance between the steel specimen and nozzle was kept constant at 3mm to enhance uniform distribution of the aluminium oxide solid particles stream **[38]**. The test machine was turned on for several minutes before each test with objective to stabilize the feed rate before each test. The AISI 1018 steel specimen is mounted on the specimen holder facing the nozzle as displayed in **Figure 1(b)**. The dry erosion tests were run at 10, 300, and 600secondsfor each of the tested impact angle and velocity. Specimens were weighed before and after each test using a digital balance with accuracy of 0.00001g to calculate the difference in weight loss.

Results

The results of AISI 1018 steel subjected to aluminium solid particles at four different velocities of 20, 40, 60 and 80m/s and impact angle of angles of 30 and 90° are presented in this section. The two angles were selected to investigate the behaviour of the AISI1018 steel at both low and high impact angles. The results obtained from SEM characterization of the eroded AISI 1018 steel surfaces are also shown and discussed.

Weight loss and erosion rate investigation

Fig. 3 shows the weight loss of AISI1018 steel after impinging with aluminium oxide particles at different velocities and angles. The results indicate that impinging the AISI1018 steel surface at 30° and different velocities (**Fig. 3a**), led to increasing weight loss compared with impinging the specimens at 90° (**Fig. 3b**). It is evident that weight loss of AISI 1018 steel at 30° is much higher than that at 90° impact angle at the same testing velocities and time, showing the influence of impact angle in material loss.

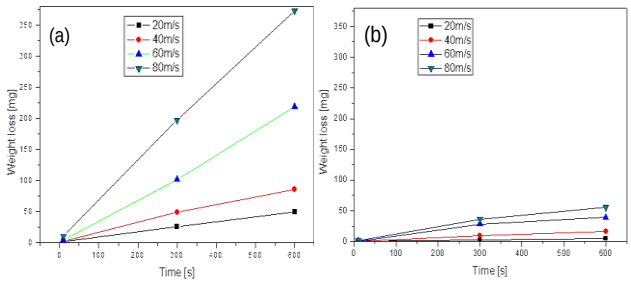

Fig. 3. The weight loss of AISI 1018 steel material at different velocities for: (a) 30° and (b) 90° impact angles.

Fig. 4 shows the erosion rate results for the four velocities at two different tested angles. The erosion rates were measured from the slope of the weight loss vs. time curves. It can be seen that the erosion rates of all AISI 1018 steels increased with increasing particle velocity for the two impact angles when the AISI 1018 steels were impinged with aluminium oxide solid particles. The results also show that the erosion rate of AISI 1018 steel impinged at 30° is higher than that impinged at 90° (**Fig. 4**).

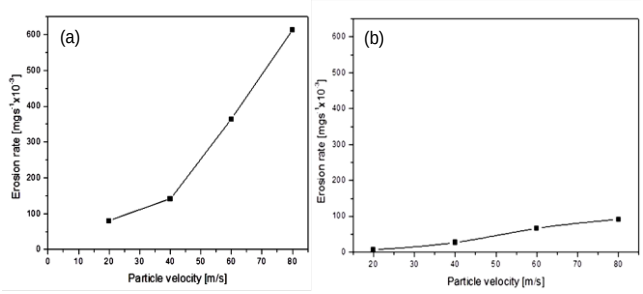

Fig. 4. The erosion rate vs particle velocity for (a) 30° impact angle and (b) 90° impact angle.

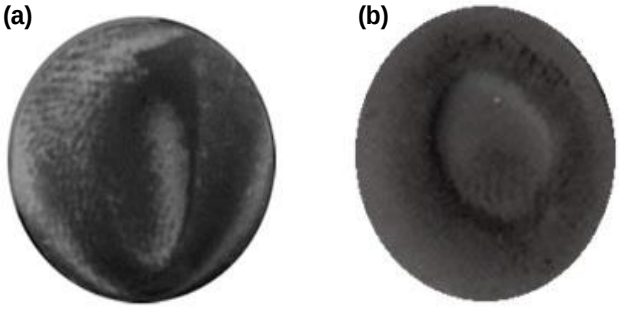

Fig. 5. Typical micrographs of AISI 1018 steel at 80m/s, 600s: (a) at 30° and (b) at 90°.

General characterization of the eroded AISI 1018 steel surfaces

Scanning electron microscope was used to show the entire eroded surface and to identify the general erosion behaviour of the AISI 1018 steel impinged by aluminium oxide particle. The lower magnification images of AISI 1018 steel at 30and 90°impact angles for 600 seconds test duration at 80m/s are shown in **Fig. 5**. The 80m/s and 600 seconds test condition was selected to display the extent of damage caused by impinging aluminium oxide particles on the AISI 1018 steel surfaces at the peak impact velocity and maximum test duration.

Fig. 5 (a) shows that the shape of eroded AISI 1018 steel surface at 30° impact angle is elliptical. This occurred as a result of divergence of high particle stream on the target steel surface at high velocity. On the other hand, **Fig. 5(b)** displays the surface scar of the eroded AISI 1018 steel impinged by aluminium oxide particle at 90°.The shape of the scar observed on the eroded surface appears circular as displayed in **Fig. 5(b)**.

Erosion mechanism characterization at 20m/s and different angles

Fig. 6(a) displays the results of the tests conducted at 20m/s and 30° impact angles for 10seconds. Micro cutting of the AISI 1018 steel surface and embedment of aluminium oxide particles on the targeted steel surface is evident. As the test duration was increased to 300 seconds under the same impact angle and velocity condition, the severity of the micro cutting mechanism increased as can be seen in **Fig. 6(b)**. Increasing the test duration to 600 seconds showed further increase in the severity of the cutting action observed on the AISI 1018 steel surface [**Fig. 6(c)**].

The SEM micrographs of the study conducted at 90° impact angles, show ploughing of the AISI 1018 steel surface for the tests performed at 20m/s for 10 seconds [**Fig. 6(d)**]. Evidence of increasing ploughing mechanism as the test duration was increased to 300 seconds was also observed as shown in [**Fig. 6(e)**].It could also be seen that the ploughing has started building up in size at some point along the ploughing [**Fig. 6(e)**]. [**Fig. 6(f)**] presents the result obtained when the test duration was increased to 600 seconds at the same velocity and angle. It could be seen that ploughing observed at this test condition has increased in width of up to 20µm [**Fig. 6(f)**].

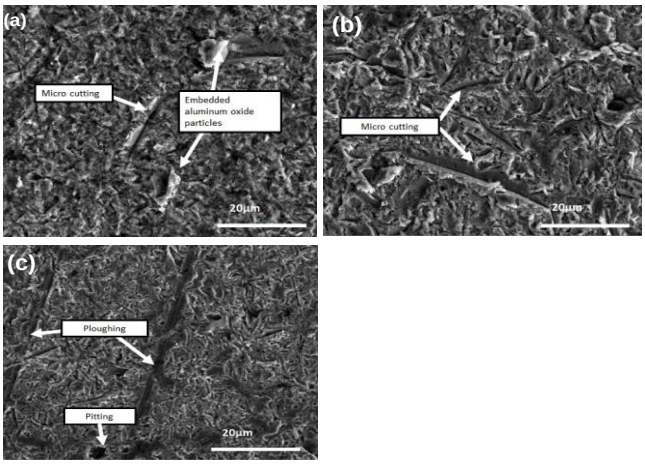

Fig. 6. SEM micrographs of 20m/s at 30° for: (a) 10s, (b) 300s and (c) 600s.

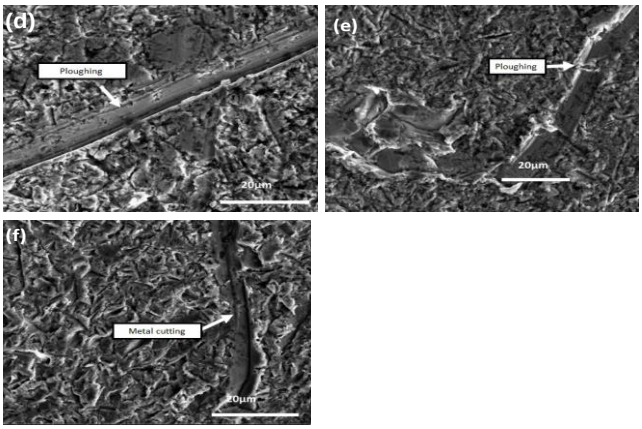

Fig. 6. SEM micrographs of 20m/s at 90° for (d) 10s, (e) 300s and (f) 600s.

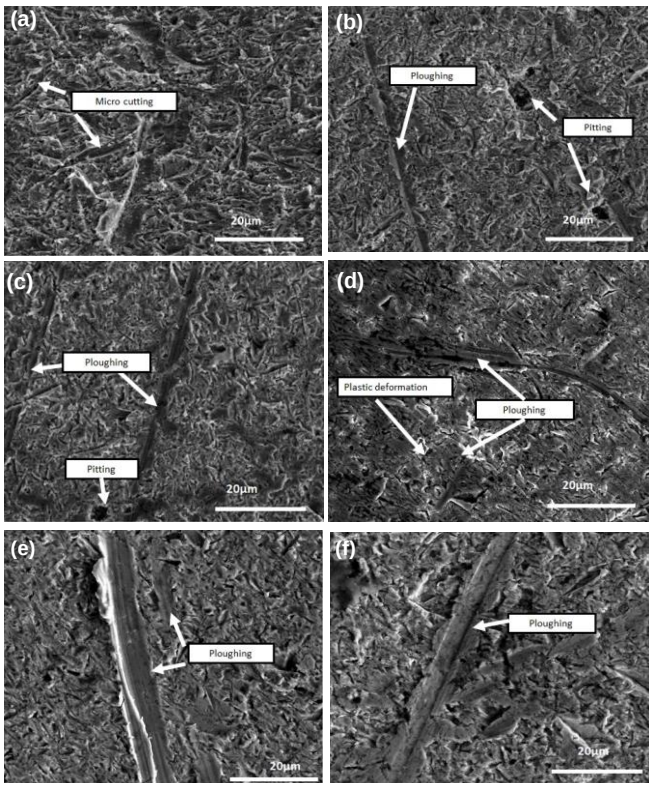

Fig. 7. SEM micrographs of 40m/s at 30° for: (a) 10s, (b) 300s (c) 600s and at 90° for: (d) 10s, (e) 300s and (f) 600s.

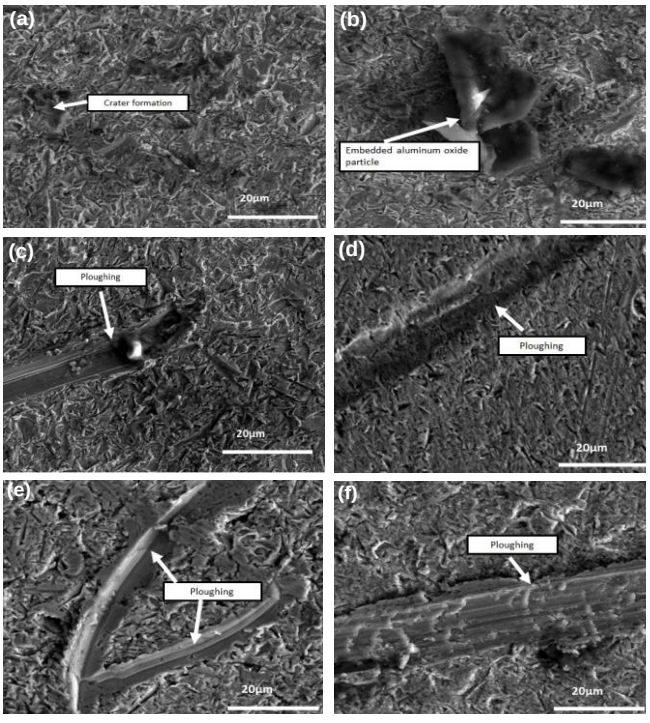

Fig. 8. SEM micrographs of 60m/s at 30° for: (a) 10s, (b) 300s (c) 600s and at 90° for: (d) 10s, (e) 300s and (f) 600s.

Erosion mechanism characterization at 40m/s and different angles

The eroded surface of AISI 1018 steel at 30° impact angle for 80m/s and 10 seconds duration is shown in (**Fig. 7(a)**). The feature observed at this test condition is typical of

micro cuttings that almost cover the entire steel surface **(Fig. 7(a))**. As the test duration was increased to 300 seconds under the same velocity, multiple ploughing and pitting of the steel surface were obvious (**Fig. 7(b)**). When the test duration was increased further to 600 seconds, similar features to that seen at 300 seconds test were observed (**Fig. 7(c)**). It implies that the mechanism did not change when the test duration was increased from 300 to 600 seconds in these tests, but increased in severity of the prevailing mechanism.

Fig. 7(d) shows the ploughing mechanism observed when the test was carried out at 60m/s and 90° impact angle for 10 seconds. At this test conditions, ploughing of the AISI 1018 steel surface was evident **(Fig. 7(d, e** and **f)**). It is also interesting to observe that the number of ploughing observed on the steel surface has increased in number as the test duration was increased to 300 seconds. When the test duration was further increased to 600 seconds at the same 90° impact angle, multiple ploughing which are bigger in sizes compared to the tests conducted at 300 seconds were evident **(Figure 7(f)**).

Erosion mechanism characterization at 60m/s and different angles

Fig. 8(a) presents the damage that occurred on AISI 1018 steel surface at 40m/s and 30° for 10 seconds. Crater formations of up to 15µm in size were observed (**Fig. 8(a)**). The SEM micrographs of the eroded specimens at 40m/s and 30° for 300 seconds show embedded aluminium oxide particle features **(Fig. 8(b)**). When the test duration was increased to 600 seconds under the same velocity and impact angle, ploughing of the steel surface was observed to be active erosive mechanism for the tests conducted at this conditions (**Fig. 8(c)**). The micrographs show that the AISI 1018 steel surface is abraded and ploughed (**Fig. 8(c)**).

The SEM micrographs of eroded AISI 1018 steel surface at 40m/s and 90° impact angle for different test durations are shown in (**Fig. 8(d-f)**). Ploughing mechanism is evident at this test conditions. There is also a distinct trend in the overall mechanism as the test duration is increased. Ploughing of about 20 µm in width was observed on the AISI 1018 steel surface at 10 seconds test duration. It is interesting to note that the number of ploughing increased when the test duration was increased to 300 seconds. Multiple ploughing of up to 12µm in width that intersect at certain point was seen at this test condition (**Fig. 8(e)**). Evidence of increased width in the observed ploughing was found when the test duration was increased to 600 seconds (**Fig. 8(f)**).

Erosion mechanism characterisation at 80m/s and different angles

The topographies of the eroded surface of specimens under various velocities at 30° impact angle are shown in **Fig. 9**. Severe plastic deformation and low angle cutting were the dominating features observed on the steel surface tested at 60m/s and 30° for 10 seconds (**Fig. 9(a)**). At longer test duration (300 seconds), multiple low angle cuttings, accompanied with embedded aluminium oxide particles were observed (**Fig. 9(b)**). The embedded aluminium oxide particle is plastically deformed as the test duration was increased to 600 seconds (**Fig. 9(c)**). Low angle cutting features, bigger in size also appeared as the test duration was increased (**Fig. 9(c)**). (**Fig. 9(d)**) shows that the ploughing mechanism is evident on the steel surface after eroded with aluminium oxide particle at 80m/s and 90° for 10 seconds. At longer test duration of 300 seconds under the same velocity and angle, multiple ploughing of the steel surface was also evident (**Fig. 9(e)**). At 80m/s, and 90° impact angle for 600 seconds, evidence of continuous multiple ploughing due to repeated aluminium oxide particles bombardment of the AISI 1018 steel surface was observed **(Fig. 9(f)**).

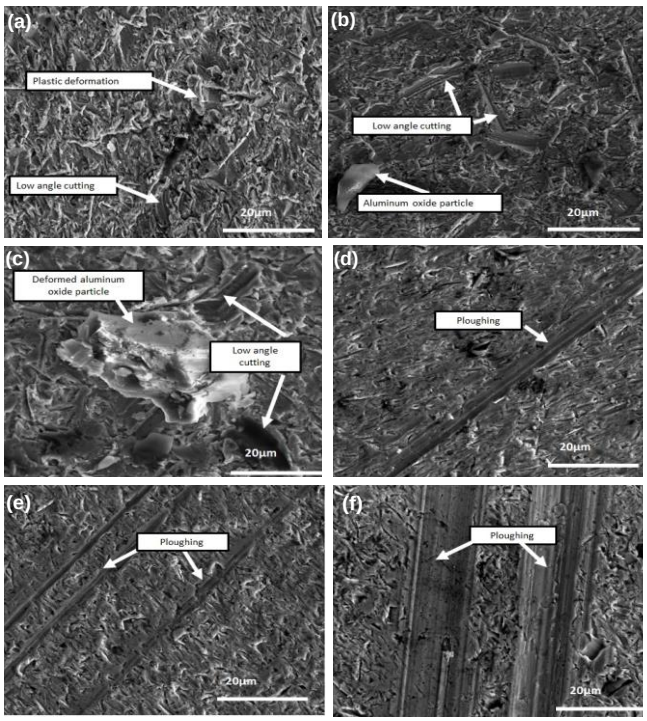

Fig. 9. SEM micrographs of 80m/s at 30° for: (a) 10s, (b) 300s (c) 600s and at 90° for: (d) 10s, (e) 300s and (f) 600s.

Discussion

The high erosion rate of AISI 1018 steel at 30° impact angle compared to 90° impact angle as the particle velocity was increased (**Fig. 3**), is typical for ductile material behaviour and is in agreement with reports by many authors**[25, 26, 32**]. Micro cutting and metal cutting features observed on the eroded surfaces at 30° impact angle and at lower velocity [**Fig. 6(a-c)** and **Fig. 7(a-c)**] suggest that material removal is the primary erosion mechanism at those test conditions. The materials removal mechanism observed at 30° impact angle and lower velocity is in agreement with the observation of Juan et al. **[39]**, who reported similar erosive mechanism of AISI 1018 steel surface at low impact angle. Other authors **[17, 26**] have reported that micro cutting and repeated plastic deformation followed by metal cutting are associated with material removal mechanisms in ductile materials as observed in this study [**Fig. 6(a-c)]**.Material removal from the target AISI 1018 steel surface through micro cutting,

pitting and ploughing became more prevalent as the velocity was increased to 40m/s at 30° impact angle. Crater formation is a feature of repeated particle impact, where the rate controlling step might be associated with the property of the target steel material **[26]**. At 60m/s and 30° impact angle, crater formation, embedment of aluminium oxide particle on the steel surface and micro-ploughing were observed [**Fig. 8(a-c)]**. Similar observation has been pointed out in other studies **[9, 17]**. This could be as a result of increasing particle velocity and low bombarding kinetic energy. Such a phenomenon was also pointed out by other researchers **[25, 31]**. Under this condition, the aluminium oxide particles are embedded into the steel matrix **[Fig. 9(b)]**. It has also been reported **[40, 41]** that metal removal under low impact angle and high velocity conditions occurs by low angle metal cutting process as observed in this study [**Fig. 9(a-c)]**. As the particles velocity was increased to 80m/s at 30° impact angle, the eroded metal surface is cut in "disc-shape" by the bombarding aluminium oxide particles. It is also well known that one surface impact on another during a repeated contact, the contact induces an alternating subsurface shear stress and plastic strain. On repeated contact, subsurface plastic strain is built up with increasing cycles resulting in formation of pits on the surfaces, as seen at 80m/s and 30° of this study.

In respect of the tests performed at 90° impact angle, evidence of ploughing in all the tests conducted at lower velocities indicate that ploughing mechanism is the operative erosion mechanism **[Fig. 6(d-f) and Fig. 7(d-f)]**. On the other hand, the SEM results of AISI 1018 steel surfaces **[Fig. 8(a-c) and Fig. 9(a-c)]** conducted at higher velocity of 90° impact angle **[Fig. 8(d-f) and Fig. 9(d-f)]** provide evidence that multiple ploughing of the steel surface were the prevailing erosion mechanisms at higher velocity test conditions. Evidently, ploughing mechanism was observed as prevailing erosive mechanism for the entire test conducted at 90° impact angle, as shown in **Fig.6, 7, 8, and 9**.Increase in particles velocity did not change the ploughing mechanism observed at high impact angle tests. It is believed that increase in the impact angle could have resulted in decrease in the ploughing mechanism as previously pointed out by other authors **[25, 41, 42]**, where it was revealed that impact angle has significant impact on the erosion mechanism of solid particles. It is also believed that at higher impact particles velocity, the elastic strain energy is high and may exceed the strain energy of the target materials**[8, 31]**. Under this condition, plastic deformation of the target surface results in micro cutting and ploughing of the target surface. For stream particle erosion process, the impinging and reflecting aluminium oxide particles may collide and the direction of the impinging particles may change**[43, 44]**, as seen in this study. When the impact angle is increased under this condition, the sliding component of the particles velocity may as well plough the target surface depending on the rotation of abrasive particles after impact on the target surface**[9, 31]**. This observation was supported by recent study of Al-Bukhaitiet al. **[25]**, where ploughing mechanism of AISI 1017 steel was observed on the target steel surface between impact angle of 15 to 75°which is in close agreement with the observation of this study. It could then be inferred that ploughing mechanism seen at 90° impact angle is influenced by material property.

In the current work, as the particles velocity is increased at the 90° impact angle, the dominant erosion mechanism of ploughing intensified with increase in the width and number of ploughings found on the AISI 1018 steel surface. This highlights the effect of impact angle and associated mechanism as the particle velocity is increased. The concept of increasing ploughing mechanism at higher impact angle has been discussed **[25]**.However, this is the first investigation using AISI 1018 steel against aluminium oxide particle under this test condition, which suggests the possibility of an optimal velocity and material property in the erosion mechanism trend of AISI 1018 steel. This result also suggest that the erosion mechanism of AISI1018 steel in oil and gas transportation pipeline could be strongly influenced by increased velocity and material property and should be considered as important factors in the erosion of oil and gas pipelines.

Conclusion

The study of the effect of particles velocity and impact angle on the erosion behaviour and mechanisms of AISI 1018 steel has led to the following conclusions:

1. The weight loss and erosion rate of AISI 1018 steel increases with increasing particle velocity for the impact angles considered in this study. The increase in weight loss and erosion rate is attributed to increasing particle penetration rate as the velocity increases.
2. SEM examinations clearly showed that ploughing mechanism occurred at different particles velocity of 90° impact angle. It was assumed that ploughing mechanism observed at 90° impact angle may be influenced by the material property.
3. Examination of the eroded AISI1018 steel surface impinged at different angles and velocities revealed that low angle metal cutting was the prevailing mechanisms at low impact angle and higher speed, while ploughing was the operative mechanism at higher impact angle.
4. The ploughing erosion mechanisms of AISI 1018 steel observed may be responsible for the failure of oil and gas steel pipeline and further study will consider selection of appropriate coating to reduce the erosion of the steel pipeline materials.

Acknowledgements
This publication was made possible by NPRP Grant 6-027-2-010 from the Qatar National Research Fund (a member of the Qatar Foundation). Statements made herein are solely the responsibility of the authors.

Reference

1. Najibi, H. et al., Applied Thermal Engineering, 2009. **29**(10): p. 2009 **DOI:** 10.1016/j.applthermaleng.2008.10.008
2. Thomas, S.;R.A. Dawe, 2003., **28**(14): p. 1461 **DOI:** 10.1016/S0360-5442(03)00124-5
3. Das, S.K.,et al.,Engineering Failure Analysis, 2014., **40**: p. 89 **DOI:** 10.1016/j.engfailanal.2014.02.015
4. Hairil Mohd,M.; J.K. Paik,2013. **67**: p. 130 **DOI:** 10.1016/j.corsci.2012.10.008
5. Postlethwaite, J.; M.H. Dobbin,;K. Bergevin, Corrosion, 1986. **42**(9): p. 514-521 10.5006/1.3583060
6. Finnie, I., Wear, 1960. **3**(2): p. 87-103 **DOI:**10.1016/0043-1648(60)90055-7

7. Neilson, J.H. and A. Gilchrist, *Erosion by a stream of solid particles.* Wear, 1968. **11**(2): p. 111-122 **DOI:**10.1016/0043-1648(68)90591-7
8. Sundararajan, G. and P.G. Shewmon, Wear, 1983. **84**(2): p. 237 **DOI:** 10.1016/0043-1648(83)90266-1
9. Hutchings, I.M., Wear, 1981. **70**(3): p. 269 **DOI:** 10.1016/0043-1648(81)90347-1
10. O'Flynn; D.J., et al., Wear, 2001. **248**(1–2): p. 162 **DOI:** 10.1016/S0043-1648(00)00554-8
11. Andrews; D.R.; J.E. Field, D: Applied Physics, 1982. **15**(11): p. 2357
12. Bousser, E., L. Martinu.; J.E. Klemberg-Sapieha, Journal of Materials Science, 2013. **48**(16): p. 5543 **DOI:** 10.1007/s10853-013-7349-y
13. Maasberg,J.A.;A.V.Levy,1981.**73**(2), **355** **DOI:** 10.1016/0043-1648(81)90300-8
14. Gat, N. and W. Tabakoff,. Wear, 1978. **50**(1), 85 **DOI:**10.1016/0043-1648(78)90247-8
15. Sundararajan, G. and M. Roy, Tribology International, 1997. **30**(5): p. 339. **DOI:** 10.1016/S0301-679X(96)00064-3
16. D. Lopez, et al., Wear, 2005. **259**: p. 118.
17. Islam, M.A. and Z.N. Farhat, Wear, 2014. **311**(1–2):,180 **DOI:** 10.1016/j.wear.2014.01.005
18. Head, W.J. and M.E. Harr, Wear, 1970. **15**(1),46 **DOI:**10.1016/0043-1648(70)90184-5
19. Wang, Y.-F. and Z.-G. Yang,2008. **265**(5–6),871 **DOI:**10.1016/j.wear.2008.01.014
20. Buijs, M. and K.K.-v. Houten, 1993. **166**(2): p. 237 **DOI:** 10.1016/0043-1648(93)90267-P
21. Evans, A.G. and T.R. Wilshaw, Acta Metallurgica, 1976. **24**(10): p. 939-956 **DOI:** 10.1016/0001-6160(76)90042-0
22. Wood, R.J.K., Wear, 2006. **261**(9): p. 1012-1023 **DOI:** 10.1016/j.wear.2006.03.033
23. Dhar, S., et al., Wear, 2005. **258**(1–4): p. 567-579 **DOI:** 10.1016/j.wear.2004.09.016
24. Stack, M.M. and N. Pungwiwat, Tribology International, 2002. **35**(10): p. 651-660. **DOI:** 10.1016/S0301-679X(02)00056-7
25. Al-Bukhaiti, M.A., et al., Wear, 2007. **262**(9–10): p. 1187-1198 **DOI:** 10.1016/j.wear.2006.11.018
26. Manisekaran, T., et al., Journal of Materials Engineering and Performance, 2007. **16**(5): p. 567-572 10.1007/s11665-007-9068-5
27. Lindsley, B.A. and A.R. Marder, *The effect of velocity on the solid particle erosion rate of alloys.* Wear, 1999. **225–229, Part 1**(0): p. 510-516 **DOI:** 10.1016/S0043-1648(99)00085-X
28. Oka, Y.I., et al., Wear, 1997. **203–204**(0): p. 573-579 **DOI:** 10.1016/S0043-1648(96)07430-3
29. Matsumura, M., et al., ISIJ International, 1991. **31**(2): p. 168-176
30. Stackwick, G.W. and A.W. Batchelor, 2001: Butterworth-Heinemann, Boston
31. Hutchings, I.M., International Journal of Mechanical Sciences, 1977. **19**(1): p. 45-52 **DOI:** 10.1016/0020-7403(77)90015-7
32. Hutchings, I.M. and R.E. Winter, Wear, 1974. **27**(1): p. 121-128 **DOI:** 10.1016/0043-1648(74)90091-X
33. Fuyan, L. and S. Hesheng, Wear, 1991. **141**(2): p. 279-289 **DOI:** 10.1016/0043-1648(91)90274-X
34. Wada, S., N. Watanabe, and T. Tani. *Solid particle erosion of brittle materials (Part 6) - The erosive wear of A.lzOa - Sic composites*. in *Yogyo Kyokai Shi*. 1987.
35. Burstein, G.T. and K. Sasaki, Wear, 2000. **240**(1–2): p. 80-94 **DOI:** 10.1016/S0043-1648(00)00344-6
36. ASTM, *Standard Test Method for Conducting Erosion Tests by Solid Particle Impingement Using Gas Jets -ASTM G76 - 13*. 2009. 03.02
37. Ruff, A.W. and l.k. Ives, Wear, 1975. **35**: p. 195-199
38. Axinte, D.A., et al., International Journal of Machine Tools and Manufacture, 2009. **49**(10): p. 797-803 **DOI:** 10.1016/j.ijmachtools.2009.04.003
39. Juan, R.L.-C., et al., *Solid Particle Erosion on Different Metallic Materials*. 2013
40. Hashish, M., Journal of Engineering Materials and Technology, 1984. **106**(1): p. 88-100 10.1115/1.3225682
41. Finnie, I., Wear, 1995. 186–187, Part 1(0): p. 1-10 **DOI:** 10.1016/0043-1648(95)07188-1
42. Finnie, I., et al., *Fundamental mechanisms of the erosive wear of ductile metals by solid particles. Discussion*. 1979, Philadelphia, PA, ETATS-UNIS: American Society for Testing and Materials. 23
43. Gomes-Ferreira, C., D. Ciampini, and M. Papini, Tribology International, 2004. **37**(10): p. 791-807
44. Shirazi, S.A. and B.S. McLaury. *Erosion modeling of elbows in multiphase flow, In: Proceedings of 2000 ASME fluids engineering summer meeting*, 2000. Boston, MA

